DOI: 10.1002/chem.200500904

Unusual High-Temperature Structural Behaviour in Ferroelectric Bi_2WO_6

Neil A. McDowell,[a] Kevin S. Knight,[b, c] and Philip Lightfoot*[a]

Abstract: The crystal structure of Aurivillius phase ferroelectric Bi_2WO_6 has been studied in detail as a function of temperature by using high-resolution powder neutron diffraction. In agreement with an earlier study, a transition from space group $P2_1ab$ to $B2cb$ occurs at about 660 °C. This transition corresponds to the loss of one octahedral tilt mode within the perovskite-like WO_4 layer of the structure. A second, reconstructive, phase transition occurs around 960 °C, corresponding to the ferroelectric Curie point; in contrast to previous suggestions, the structure of this high-temperature phase contains layers of stoichiometry WO_4, with WO_6 octahedra sharing edges and corners, and with the fluorite-like Bi_2O_2 layers remaining essentially unchanged. This structure is closely related to that of the ambient temperature phase of lanthanide-doped derivatives, for example, $Bi_{0.7}Yb_{1.3}WO_6$ recently reported. This phase-transition behaviour is in stark contrast to that of other members of the Aurivillius family, such as $SrBi_2Ta_2O_9$ and $Bi_4Ti_3O_{12}$, which retain the archetypal Aurivillius connectivity at all temperatures.

Keywords: bismuth oxide · ferroelectric · neutron diffraction · perovskite phases · phase transitions · tungsten

Introduction

Bi_2WO_6 is an archetypal $n=1$ member of the Aurivillius family of layered perovskites, which are structurally composed of alternating perovskite-like and fluorite-like blocks, of general formula $[Bi_2O_2][A_{n-1}B_nO_{3n+1}]$.[1] For Bi_2WO_6 the perovskite block consists of an infinite two-dimensional array of corner-linked WO_6 octahedra, one octahedral layer thick. The crystal structure of the ambient-temperature phase of Bi_2WO_6 has been studied in detail using both single-crystal X-ray diffraction (XRD)[2] and high-resolution powder neutron diffraction (PND).[3] Both studies agree on the assignment of the polar space group $P2_1ab$ (No. 29) to this phase (hereafter referred to as the low-temperature (LT) phase, in contrast to earlier work, which suggested the higher symmetry $B2cb$ (No. 41).[4]

Bi_2WO_6 is a well-known ferroelectric compound with a high Curie temperature ($T_C \sim 960$ °C).[5] In addition to the paraelectric–ferroelectric phase transition, it has been suggested by several authors that a second structural phase transition exists, at a temperature of about 660 °C.[6,7] Watanabe[6] used dilatometric and differential thermal analysis (DTA) measurements to suggest an intermediate phase change with very small enthalpy and change in dimensionality of the crystals; Yanovskii and Voronkova[7] quantified this somewhat further by carrying out a high-temperature powder XRD study and suggested a second polar orthorhombic phase at approximately $690\,°C < T < 960\,°C$. Knight has studied this intermediate temperature (IT) phase in detail using PND,[8] and established unequivocally that the material in this temperature regime adopts the orthorhombic $B2cb$ space group, and retains the essential Aurivillius structure, albeit losing one "tilt" mode of the perovskite-like octahedral layer.

Although all the previous authors have been aware of the existence of the additional high-temperature (HT) phase ($T > 960$ °C), it has so far eluded a definitive structural characterisation. Watanabe identified a marked similarity of the X-ray powder pattern of this high-temperature phase to that of $BiLaWO_6$. Based on previous work on that phase, using high-resolution electron microscopy and Raman spectra, Watanabe had tentatively suggested[9] an unusual layered-

[a] N. A. McDowell, Dr. P. Lightfoot
EaStChem, School of Chemistry
University of St. Andrews
St.Andrews, KY16 9ST (UK)
Fax: (+44) 1334-463-808
E-mail: pl@st-and.ac.uk

[b] Dr. K. S. Knight
ISIS Facility, Rutherford Appleton Laboratory
Chilton, Oxon, OX11 0QX (UK)

[c] Dr. K. S. Knight
Department of Mineralogy, The Natural History Museum
Cromwell Road, London, SW7 5BD (UK)

Supporting information for this article is available on the WWW under http://www.chemeurj.org/ or from the author.

type structure, in a monoclinic unit cell, which retained the fluorite-like Bi_2O_2 layers of the parent phase but reconstructed the perovskite-like layer of corner-sharing WO_6 octahedra to isolated WO_4 tetrahedra, whilst still retaining the overall WO_4 stoichiometry. Our own recent work[10] on isostructural $Bi_{0.7}Yb_{1.3}WO_6$ has shown this model to be incorrect; this phase contains WO_4 layers consisting of dimeric chains of edge-sharing WO_6 octahedra, rather than either corner sharing octahedra or isolated tetrahedra.

In order to clarify the full high-temperature phase diagram of Bi_2WO_6 we have carried out a further PND study, in which we highlight further details of the thermal evolution of the LT and IT phases, and also confirm that the long misunderstood HT phase does indeed correspond to $BiLaWO_6$, consisting of alternating layers of fluorite-like Bi_2O_2 and edge-sharing octahedral chains of WO_4 stioichiometry.

Experimental Section

A yellow polycrystalline sample of Bi_2WO_6 (approximately 10 g) was prepared by heating a thoroughly ground stoichiometric mixture of Bi_2O_3 and WO_3 at 750 °C for 48 h, followed by heating at 850 °C for 24 h, with one intermediate regrinding. Phase purity was confirmed by X-ray powder diffraction. Powder neutron diffraction data were collected on the high-resolution time-of-flight powder diffractometer (HRPD) at ISIS, Rutherford Appleton Laboratory. The sample was first sealed under vacuum in a thin-walled silica tube, to prevent volatilisation at elevated temperatures, and then loaded into a cylindrical vanadium can. PND data were collected at temperatures of 20 and 100 °C, then at 25 °C intervals to 600 °C, 10 °C intervals to 700 °C, 25 °C intervals to 900 °C, and 10 °C intervals to 960 °C. The standard data-collection time was about 15 minutes (8 μA h) at each temperature, with longer runs of about 4.5 h (150 μAhr) at temperatures of 400, 800 and 900 °C in order to define the LT and IT phases. A final 150 μAhr dataset was collected at 965 °C once complete transformation to the HT phase had been confirmed. Data from two detector banks, at $2\theta \sim 168$ and 90°, were used in subsequent Rietveld analysis using the general structural analysis system (GSAS) package.[11] An appropriate cylindrical absorption correction was applied to all datasets. Further details of the data collection and refinement are given in Table 1.

Table 1. Details of neutron data collection and refinement.

Temperature [°C]	400	900	965
space group	$P2_1ab$	$B2cb$	$A2/m$
a [Å]	5.48806(3)	5.53422(2)	8.37445(5)
b [Å]	5.46073(2)	5.49995(2)	3.85444(2)
c [Å]	16.48455(8)	16.55045(7)	16.4403(1)
β [°]			102.334(1)
data range [Å]	0.7–3.2	0.7–3.2	0.85–3.5
contributing reflections	809	417	525
no. parameters	60	64	49
Rwp, Rp	0.042, 0.040	0.036, 0.034	0.044, 0.042

Results and Discussion

Thermal evolution of the Aurivillius structure: In the previous PND study,[8] a full structural characterisation versus temperature was not carried out. Instead, the evolution of lattice parameters and space group was ascertained by a model-independent profile fit, and the structure of the IT phase was determined at only one temperature (688 °C). In the present study we extend this work to establish detailed structural models at all temperatures. In line with the previous work, all datasets up to 660 °C were refined using the $P2_1ab$ space group; in this study we choose the nonstandard setting of $Pca2_1$ (No. 29) in order to conform with the convention in Aurivillius phase ferroelectrics of assigning the "long" axis as c, and the polar axis as a. Around the anticipated LT–IT phase transition, a careful comparison of fits in both $P2_1ab$ and $B2cb$ (nonstandard setting of $Aba2$, No. 41) was undertaken. In particular, the observation of key reflections violating B-centring was noted at 660 °C. It was confirmed that the transition occurs at this point, with $P2_1ab$ being the best description of the structure at 660 °C and $B2cb$ the best description at 670 °C. The $B2cb$ (IT) structure is maintained up to 950 °C, with evidence of a slow (i.e., first-order) phase transition at 960 °C, involving temporary coexistence of the two phases, which is complete at 965 °C (HT phase). By using these two models for the Aurivillius structure, the Rietveld refinements proceeded smoothly with a total of 59 variables (two scale factors, 12 background parameters, diffractometer constant and six profile coefficients for the two histograms, plus three lattice parameters, 26 variable coordinates and 9 isotropic displacement parameters) for the LT, $P2_1ab$ structure and 64 variables for the IT, $B2cb$ structure. Note that the IT structure was refined anisotropically, whereas the LT structure was refined isotropically, due to the strong degree of pseudosymmetry. Further details of these refinements are given in Table 1. Representative Rietveld fits for the two phases are given in Figure 1, with selected tables of final refined atomic parameters being provided in the Supporting Information. Note that the anisotropic atomic displacement parameters for the IT phase are consistent with the anticipated thermal motion of the WO_6 polyhedra. Selected bond lengths and angles for the two datasets at 400 and 900 °C are given in Table 2, with the corresponding atom-numbering scheme shown in Figure 2.

Thermal evolution of the lattice parameters for these two phases is shown in Figure 3. The trends agree with those in the previous PND study,[8] with clear evidence of a phase transition at 660 °C. It is interesting to note that the deviation from tetragonal symmetry (Figure 3c) increases throughout the LT–IT regime, which contrasts with the behaviour seen in all previously studied Aurivillius phases, as discussed later. Mean axial thermal expansion coefficients (α) for the LT and IT phases are LT (125–630 °C): $\alpha_a = 16.8 \times 10^{-6}$, $\alpha_b = 13.9 \times 10^{-6}$, $\alpha_c = 8.6 \times 10^{-6}$ °C^{-1}; IT (725–900 °C): $\alpha_a = 10.3 \times 10^{-6}$, $\alpha_b = 9.0 \times 10^{-6}$, $\alpha_c = 9.5 \times 10^{-6}$ °C^{-1}.

To further explore the subtle evolution of the Aurivillius structure from LT to IT, it is necessary to understand the differences between the two structures, which are largely manifested in the behaviour of the perovskite-like WO_4

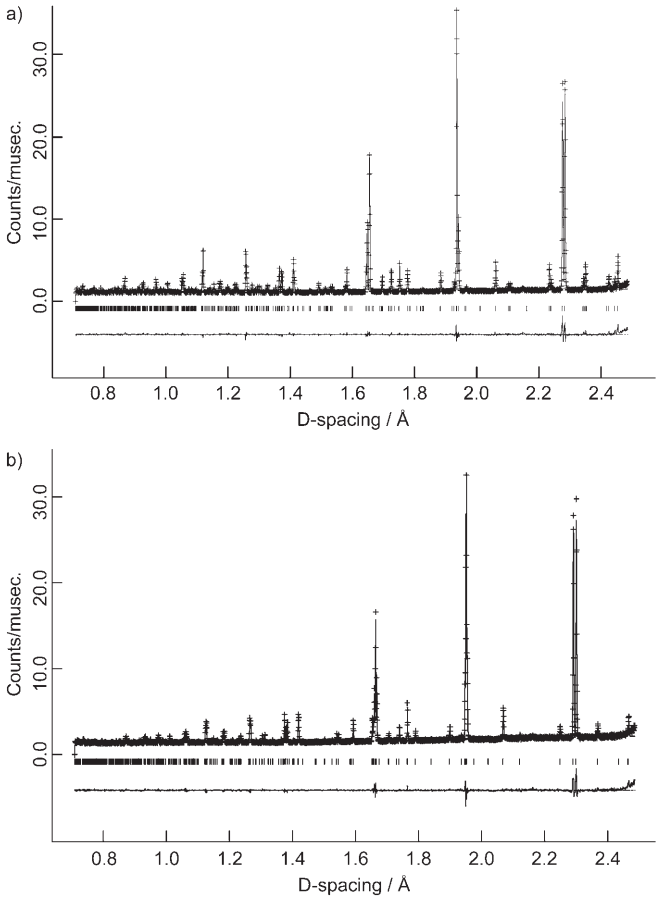

Figure 1. a) Final Rietveld fit for the LT phase, $P2_1ab$, at 400 °C. b) Final Rietveld fit for the IT phase, $B2cb$, at 900 °C.

Table 2. Selected bond lengths [Å] and angles [°] for Bi_2WO_6 in the LT (400 °C) and IT (900 °C) phases.

At 400 °C			
Bi1–O3	2.543(6)	Bi2–O2	2.228(6)
Bi1–O3	2.164(7)	Bi2–O2	2.205(8)
Bi1–O3	2.248(6)	Bi2–O2	2.502(7)
Bi1–O3	2.349(7)	W1–O1	1.85(1)
Bi1–O5	3.036(7)	W1–O4	2.240(7)
Bi1–O6	2.533(7)	W1–O4	1.728(6)
Bi1–O6	2.571(8)	W1–O5	2.215(6)
Bi2–O1	2.639(9)	W1–O5	1.720(7)
Bi2–O1	2.464(9)	W1–O6	1.87(1)
Bi2–O2	2.377(6)		
Bi2-O2-Bi2	109.4(2)	Bi1-O3-Bi1	105.5(2)
Bi2-O2-Bi2	109.7(3)	Bi1-O3-Bi1	114.0(3)
Bi2-O2-Bi2	100.2(3)	Bi1-O3-Bi1	99.6(3)
Bi2-O2-Bi2	115.3(4)	Bi1-O3-Bi1	115.8(3)
Bi2-O2-Bi2	115.3(3)	Bi1-O3-Bi1	111.3(3)
Bi2-O2-Bi2	105.8(2)	Bi1-O3-Bi1	109.5(2)
W1-O4-W1	164.2(6)	W1-O5-W1	151.1(4)
At 900 °C			
Bi1–O1	2.711(3)	Bi1–O2	2.213(5)
Bi1–O1	2.553(3)	W1–O1×2	1.861(3)
Bi1–O2	2.398(4)	W1–O3×2	2.191(5)
Bi1–O2	2.500(5)	W1–O3×2	1.738(5)
Bi1–O2	2.258(5)		
Bi1-O2-Bi1	100.5(1)	Bi1-O2-Bi1	106.6(2)
Bi1-O2-Bi1	108.6(2)	Bi1-O2-Bi1	114.8(2)
Bi1-O2-Bi1	111.5(2)	W1-O3-W1	166.3(3)
Bi1-O2-Bi1	114.0(2)		

layer. Figure 4 shows a view of this layer for both phases, a network of corner-linked WO_6 octahedra, with W being displaced noticeably towards one octahedral edge. In the LT phase there is rotation of the octahedra around both the *a* and *c* axes, but not around the *b* axis; in the IT phase there is rotation around the *a* axis only. Therefore, a measure of the LT–IT transition is the degree of rotation of the WO_6 octahedra around the *c* axis. This can be defined by taking the angle between the O4–O4 "octahedral edge" and the *a* axis within the LT phase; the corresponding O3–O3 angle in the IT phase is zero. This parameter is plotted as a function of temperature in Figure 5; the nature of this evolution is consistent with a second order LT–IT phase transition, as allowed by group theory.

In the IT phase, the tilt around the *c* axis is frozen out, but the *a* tilt persists. A measure of the evolution of this aspect of the structure between the two phases is the angle between neighbouring octahedral edges propagating along the *b* axis, within the *ab* plane, as shown in Figure 4. For the LT structure this is the angle $O4^{i}$-$O5^{i}$-$O4^{ii}$ (symmetry operators: i) *x*,*y*,*z*; ii) *x*, $-1+y$, *z*) and for the IT structure $O3^{i}$-$O3^{ii}$-$O3^{iii}$ (symmetry operators: i) x, 2-y, 2-z; ii) x,y,z; iii) x, 1−y, 2−z). Thermal evolution of this parameter is shown in Figure 6. Note that this parameter is influenced by both *a* and *c* axis tilts in the LT phase, but purely by the *a* axis tilt in the IT phase. It can be seen that, in the LT phase, this angle is relatively invariant with *T*, despite the fact that the

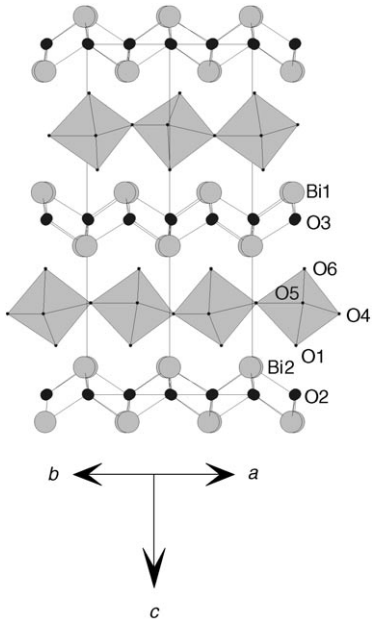

Figure 2. Crystal structure of the LT phase ($P2_1ab$). Note that in the IT phase ($B2cb$) the following pairs of atoms become crystallographically equivalent, with the IT phase numbering scheme in brackets: Bi1/Bi2 (Bi1), O1/O6 (O1), O2/O3 (O2), O4/O5 (O3).

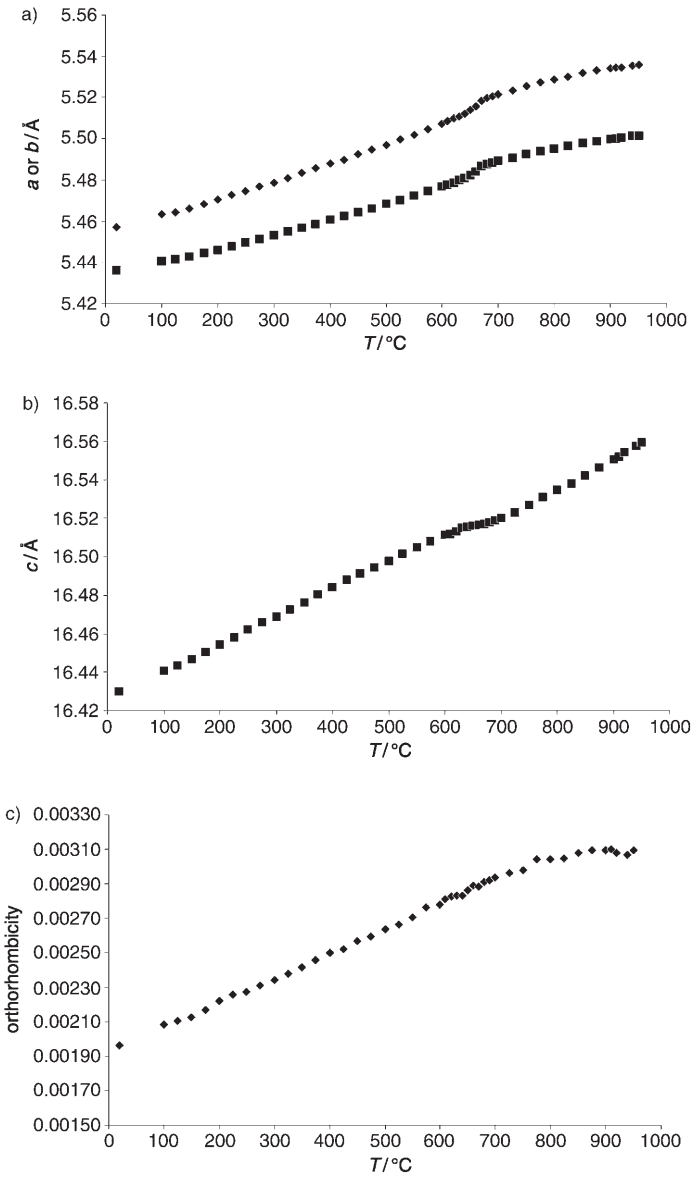

Figure 3. Thermal evolution of the lattice parameters of the Aurivillius structure through the LT–IT phase transition. a) a ◆ and b ■ axes, b) c axis, c) orthorhombic distortion $(a-b)/(a+b)$.

"c-axis tilt" mechanism described above is taking place. In other words, the change in the degree of the "a-axis tilt" is small compared to that of the c axis, on passing from the LT to the IT phase; this can be clearly seen in Figure 4. This suggests that the most straightforward way of visualising the overall evolution of the Aurivillius structure within the LT–IT regime is a two-step process, involving an essentially 2D "untilting" around the c axis in the LT regime, followed by an almost independent untilting around the a axis in the IT regime. The expected change of behaviour is seen around 660 °C, at the LT–IT transition. More subtly, and perhaps more curiously, a second change in slope is seen around 850 °C; we are currently unable to explain this feature. Between 850 and 960 °C the $O3^{i}$-$O3^{ii}$-$O3^{iii}$ angle rapidly relaxes outwards, but never reaches 180°, as would be expected if a transition towards a tetragonal paraelectric phase occurred. Instead, the observed reconstructive phase transition to the HT phase occurs.

This type of HT phase transition is unique among Aurivillius phase ferroelectrics. In previous studies of $n=2$, 3 and 4 Aurivillius phases, three different types of phase-transition sequence have been observed. Firstly, a direct, first-order transition from polar orthorhombic to centrosymmetric tetragonal at T_C, as seen in $Bi_4Ti_3O_{12}$.[12,13] Secondly, a continuous transition from polar orthorhombic to centrosymmetric orthorhombic at T_C, followed by a second transition to centrosymmetric tetragonal above T_C; this corresponds to successive freezing out of two different octahedral tilt modes, and has been observed in $SrBi_2Ta_2O_9$ and related compositions,[14,15] and $SrBi_4Ti_4O_{15}$.[16] Finally, an apparently direct transition from polar orthorhombic to centrosymmetric tetragonal at T_C; this type of transition is required to be first-order by group theory and is still the subject of some controversy.[17,18]

Crystal structure of the HT phase: In the earlier work of Watanabe[6] it was postulated that the crystal structure of HT-Bi_2WO_6 was isomorphous to that of the ambient-temperature structure of the lanthanide-doped derivatives $Bi_{2-x}Ln_xWO_6$ (approximate composition limits $0.3<x<1.3$ for most lanthanides).[19] As outlined in the Introduction, Watanabe's suggested structure of this phase has been shown to be erroneous, and the true structure has recently been established.[10] This model was therefore used as the basis for the present determination of the structure of the HT phase. Berdonosov et al.[10] lowered the symmetry of this phase from $A2/m$ to $A2$ with a significant improvement in fit. We found this to be unnecessary in the present case, and the final model for HT-Bi_2WO_6 has been carried out in $A2/m$ with no disorder of oxygen atoms. A further, more extensive, structural study of some of the $Bi_{2-x}Ln_xWO_6$ series is underway, and will be published in due course.

The final Rietveld refinement for the present model consisted of 49 parameters, with an excellent profile fit being achieved (Table 1 and Figure 7). Final structural parameters are given in Table 3 and selected geometry in Table 4. The crystal structure (Figure 8) reveals features reminiscent of the parent Aurivillius phase, namely a layered structure of alternating fluorite-like layers and layers of composition WO_4. However, there is a major reconstruction of the WO_4 layer from corner-shared octahedral sheets to edge-shared dimeric chains (Figure 9). On the other hand, the fluorite-like Bi_2O_2 layers retain a quite regular geometry, similar to those in the Aurivillius phases, although there is a significant "stretching" of this layer along the a axis, in order to accommodate the reconstruction of the WO_4 layer. Note the one extreme Bi1-O2-Bi2 angle (133.9°) in Table 4, which corresponds to alternating Bi1–Bi2 distances of 4.43 and 3.95 Å along the a axis, compared to 3.85 Å along the b axis; the corresponding distances in the IT phase at 900 °C are 3.80 and 4.00 Å along both axes. In the LT and IT Aurivillius structures the W atom is offset significantly towards one

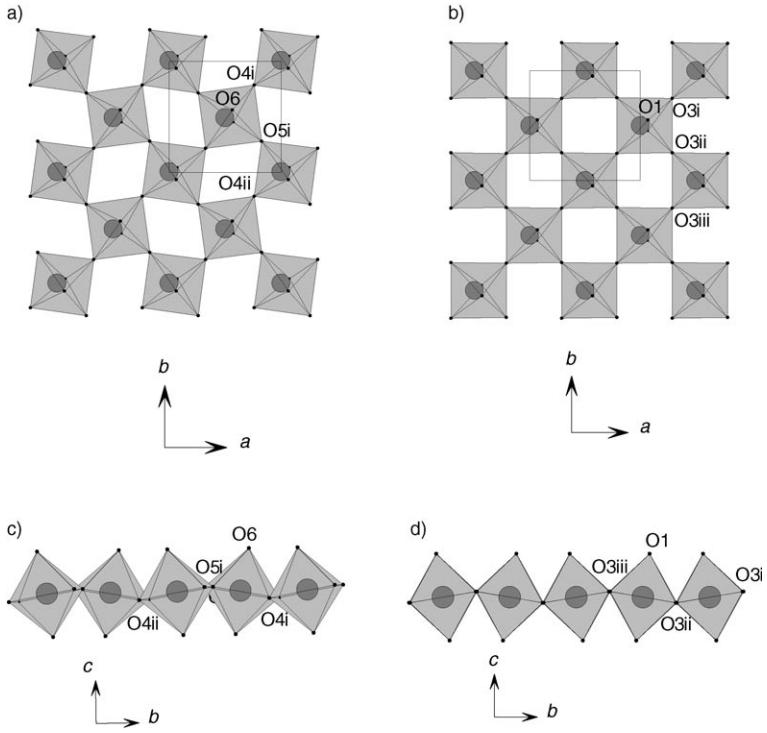

Figure 4. Views of the [WO_4] layer in a) the LT phase along [001], b) the IT phase along [001], c) the LT phase along [100], and d) the IT phase along [100].

tion between the Bi_2O_2 and WO_4 layers, the environments of the two crystallographically distinct Bi sites in this phase are significantly different than in the Aurivillius phases, as in this case Bi1 and Bi2 lie above a "gap" or above a "shared edge", respectively in the WO_4 layer. The latter case results in a significantly shorter contact than the former (Bi2–O4 = 2.583 Å, Bi1–O5 = 2.754 Å).

Conclusion

A detailed study of the high-temperature phases of Bi_2WO_6 has been carried out. The LT and IT phases are ferroelectric, and adopt polar versions of the basic Aurivillius structure, in space groups $P2_1ab$ and $B2cb$, respectively, in agreement with earlier studies.[2,3,8] The evolution of these two structures, with consecutive loss of octahedral tilt modes around the *c* and *a* axes, has been followed in detail. However, before the *a*-axis tilt is lost completely in a continuous manner, a major reconstructive phase transition to the HT phase occurs, at $T_C \sim 960\,°C$, coinciding with the loss of ferroelectricity. This HT phase adopts a layer structure with similarities, but also dramatic differences, to the Aurivillius structures, with the WO_4 layers being transformed from corner-sharing octahedral sheets to edge-sharing octahedral chains. This type of ferroelectric–paraelectric transition is unique amongst Aurivillius phases. Moreover, we are unaware of any other layered perovskite-like struc-

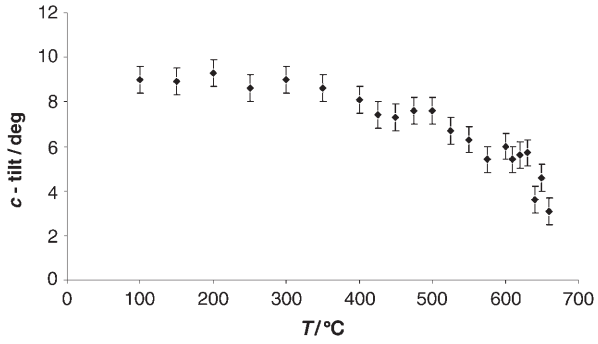

Figure 5. Thermal evolution of the angle of the O4–O4 vector versus the *a* axis within the LT phase: a measure of the tilt of the WO_6 octahedra around the *c* axis.

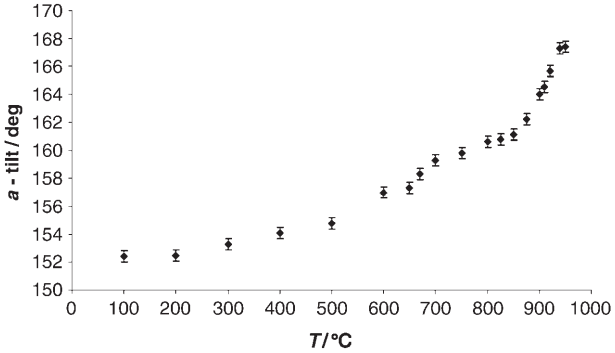

Figure 6. Thermal evolution of the angle of the O-O-O interoctahedral angle within the *ab* plane (see text and Figure 4 for definitions). This provides a measure of the tilt of the WO_6 octahedra around the *a* and *c* axes in the LT phase, and around the *a* axis only in the IT phase.

edge of the WO_6 octahedron along the polar axis; indeed, this is the major cause of the ferroelectric polarisation itself.[20] Off-centre octahedral distortions are a general feature of the structural chemistry of d^0 metal cations, a phenomenon which is generally ascribed to covalency effects (i.e., second-order Jahn–Teller effects); the specific preference of W^{6+} for edge- or face-directed displacements rather than vertex-directed is discussed by Halasyamani.[21] In the HT phase, there is no net polarisation, but within each edge-sharing dimer the W atom is once again off-centred—in this case away from the shared edge, as may be expected due to inter-cation repulsions; the W–W contact within the dimeric pair is still short, at 3.32 Å. Regarding communica-

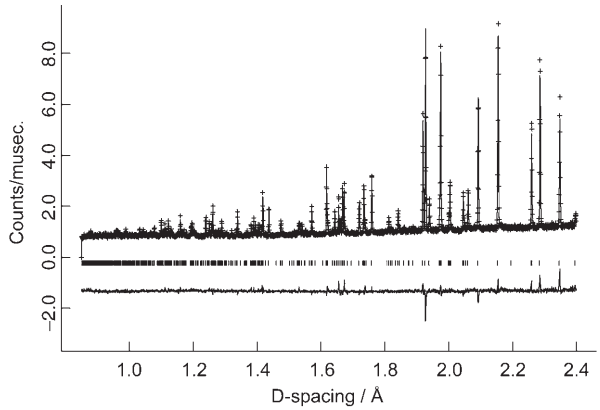

Figure 7. Final Rietveld fit for the HT phase, A2/m, at 965 °C.

Table 3. Final refined atomic parameters for Bi_2WO_6 in the HT phase (965 °C).

Atom	x	y	z	$U_{iso} \times 100$ [Å^2]
Bi1	0.9313(2)	0	0.3341(2)	4.3(1)
Bi2	0.3950(3)	0	0.3213(2)	4.7(1)
W1	0.3007(4)	0.5	0.4981(3)	2.8(1)
O1	0.1170(4)	0	0.2469(2)	4.6(1)
O2	0.3638(5)	0.5	0.2313(2)	4.5(1)
O3	0.3113(5)	0	0.4946(3)	8.0(2)
O4	0.5087(5)	0.5	0.5753(3)	5.6(1)
O5	0.1734(5)	0.5	0.5696(3)	6.6(1)
O6	0.1645(5)	0.5	0.3972(3)	7.2(2)

Table 4. Selected bond lengths [Å] and angles [°] for Bi_2WO_6 in the HT phase (965 °C).

Bi1−O1	2.331(4)	Bi2−O2	2.361(5)
Bi1−O1 × 2	2.328(3)	Bi2−O4 × 2	2.583(3)
Bi1−O2	2.475(4)	W1−O3 × 2	1.931(1)
Bi1−O5 × 2	2.754(4)	W1−O4	1.923(5)
Bi1−O6 × 2	2.782(4)	W1−O4	2.196(7)
Bi2−O1	2.387(4)	W1−O5	1.748(7)
Bi2−O2 × 2	2.409(3)	W1−O6	1.801(7)
Bi1-O1-Bi1 × 2	107.1(1)	Bi1-O2-Bi2 × 2	103.5(1)
Bi1-O1-Bi2	113.0(2)	Bi1-O2-Bi2	133.9(2)
Bi1-O1-Bi1	111.8(2)	Bi2-O2-Bi2	106.2(2)
Bi1-O1-Bi2 × 2	108.9(1)	Bi2-O2-Bi2 × 2	103.6(1)
W1-O3-W1	173.2(2)	W1-O4-W1	107.4(2)

tures that contain edge-sharing dimeric chains of the type seen in HT-Bi_2WO_6 and $Bi_{2-x}Ln_xWO_6$. The underlying reasons for this unusual behaviour merit further study.

Further details of the crystal structure investigations can be obtained from the Fachinformationszentrum Karlsruhe, 76344 Eggenstein-Leopoldshafen, Germany (fax: (+49) 7247-808-666; e-mail: crysdata@fiz.karlsruhe.de) on quoting the depository number CSD-415669.

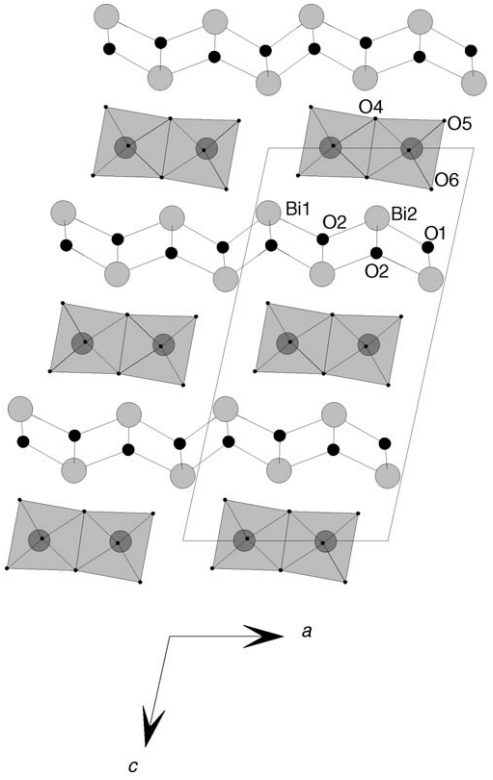

Figure 8. Crystal structure of the HT phase at 965 °C. Compare and contrast the Aurivillius structure in Figure 2.

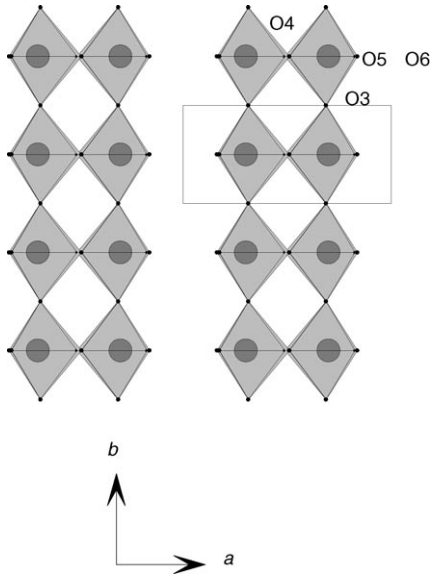

Figure 9. Plan view (along [001]) of a single [WO_4] sheet in the HT structure, showing corner-linked chains of edge-shared octahedral dimers. Compare with the perovskite-like layers shown in Figure 4a and b.

Acknowledgements

We would like to thank CCLRC for provision of neutron diffraction facilities.

[1] B. Aurivillius, *Arkiv. Kemi* **1952**, *5*, 39.
[2] A. D. Rae, J. G. Thompson, R. L. Withers, *Acta Crystallogr Sect. B.* **1991**, *47*, 870.
[3] K. S. Knight, *Min. Mag.* **1992**, *56*, 399.
[4] R. W. Wolfe, R. E. Newnham, M. I. Kay, *Solid State Commun.* **1969**, *7*, 1797.
[5] I. G. Ismailzade, F. A. Mirishli, *Kristallografiya* **1970**, *14*, 738.
[6] A. Watanabe, *J. Solid State Chem.* **1982**, *41*, 160.
[7] V. K. Yanovskii, V. I. Voronkova, *Phys. Status Solidi A* **1986**, *93*, 57.
[8] K. S. Knight, *Ferroelectrics* **1993**, *150*, 319.
[9] A. Watanabe, Y. Sekikawa, F. Izumi, *J. Solid State Chem.* **1982**, *41*, 138.
[10] P. S. Berdonosov, D. O. Charkin, V. A. Dolgikh, S. Yu. Stefanovich, R. I. Smith, P. Lightfoot, *J. Solid State Chem.* **2004**, *177*, 2632.
[11] A. C. Larson, R. B. Von Dreele, Los Alamos National Laboratory Report No. LA-UR-86-748, **1987**.
[12] E. C. Subba Rao, *Phys. Rev.* **1961**, *122*, 804.
[13] C. H. Hervoches, P. Lightfoot, in the *Proceedings of the 10th International Ceramics Congress-Part D, Advances in Science and Technology*, *Vol. 33* (Ed.: P. Vincenzini), Techna, **2003**, pp. 623–630.
[14] C. H. Hervoches, J. T. S. Irvine, P. Lightfoot, *Phys. Rev. B* **2001**, *64*, 100102(R).
[15] R. Macquart, B. J. Kennedy, B. A. Hunter, C. J. Howard, Y. Shimakawa, *Integr. Ferroelectr.* **2002**, *44*, 101.
[16] C. H. Hervoches, A. Snedden, R. Riggs, S. H. Kilcoyne, P. Manuel, P. Lightfoot, *J. Solid State Chem.* **2002**, *164*, 280.
[17] A. Snedden, C. H. Hervoches, P. Lightfoot, *Phys. Rev. B.* **2003**, *67*, 092102.
[18] N. C. Hyatt, I. M. Reaney, K. S. Knight, *Phys. Rev. B* **2005**, *71*, 024119.
[19] A. Watanabe, *Mater. Res. Bull.* **1980**, *15*, 1473.
[20] R. L. Withers, J. G. Thompson, A. D. Rae, *J. Solid State Chem.* **1991**, *94*, 404.
[21] P. S. Halasyamani, *Chem. Mater.* **2004**, *16*, 3586.

Received: July 27, 2005
Published online: November 28, 2005

